Selective ethylene removal in industrial fruit conservation chambers

Hugo Lopes

Supervisors: Prof. Dr. Maria Filipa Gomes Ribeiro[a] and Prof. Dr. Ana Cristina Ferreira de Oliveira Rodrigues[b]

[a] Centro de Química Estrutural, Instituto Superior Técnico, Universidade de Lisboa, Av. Rovisco Pais, Lisboa 1049-001, Portugal

[b] Escola Superior de Saúde, Instituto Politécnico de Leiria, Morro do Lena, Alto do Vieiro, Leiria 2411-901, Portugal

Abstract

Silver and copper-based ZSM-5 zeolites were developed to enable effective ethylene adsorption and regulation of ethylene concentration in industrial fruit storage chambers. Metal-loaded zeolite samples were subjected to breakthrough adsorption studies performed under dry and wet conditions (similar to industrial storage chambers). Shaped zeolite samples were subjected to breakthrough adsorption and adsorption-desorption tests in wet conditions. The latter experiments were conducted under "real-world" conditions in a pilot-scale adsorption system implemented in the Rocha-Center's test storage chambers. The abundance of dispersed stabilized cations (Ag^+, Cu^+) capable of interacting with ethylene through π-complexations is directly correlated with ethylene adsorption efficiency. Lower adsorption capabilities were found for Cu-based zeolites due to the stabilization of species (Cu^{2+}) incapable of interacting with ethylene through chemisorption (π-complexations). In summary, increasing the silver loading improved ethylene adsorption by increasing the number of active π-complexation species (Ag^+). Water addition, on the other hand, resulted in a large drop in adsorption capabilities (about 75%), owing to the competing adsorption of water and ethylene. The hydrophobic nature of zeolite samples with greater Si/Al ratios minimized this influence. Shaping had a significant adsorption influence, which was attributable to a reduction of active zeolite area for Ag^+ stabilization. The outcome is related to a decrease in microporosity caused by binder aggregation on the zeolite pores. Because of the proven decreased loss in microporosity, an increase in zeolite percentage resulted in improved adsorption capabilities. The regeneration characteristics of adsorbents were proven under low-temperature desorption treatment, with adsorbents recovering the majority of their performance from cycle to cycle. The experiments in the pilot scale system highlighted the efficient selective adsorption of ethylene under real-world conditions (16.3% drop in ethylene concentration after 8 hours with 3.5 g of silver extrudates) and regenerative properties of the prepared samples, as well as their mechanical properties.

Keywords- adsorption, ethylene, shaping, silver, zeolites, ZSM-5, π-complexation.

1.Introduction

Fresh fruit and vegetable production plays a crucial role in the EU's socioeconomic landscape, accounting for 13.9% of total agricultural output value with a devoted area of 5.6 million hectares. The economic and political nature of the European Union encourages the trade market for fresh products among its members (€36.8 billion fresh items transported among EU countries), although the market balance is shifting toward the importation of fresh goods. The fruit and vegetable market is heavily reliant on the maturation process, either before or after harvest, because fruit and vegetables continue to execute the majority of metabolic processes after being picked up. Thus, regulating these processes is critical to meeting market demands without incurring significant losses.

The majority of the losses are caused by water loss, microbial activity, and the generation of ethylene during storage. Ethylene is a phytohormone generated by fresh foods that is responsible for ripening and senescence. Ripening is an important stage in the development of fruits because it develops the desired market characteristics (colour, taste, scent, and texture). Ethylene, while being responsible for the ripening process, has an important role in the fresh goods production landscape. Ethylene production is related to metabolic reactions, thus low temperatures and controlled gas compositions are important to mitigate this hormone production. These conditions limit ethylene generation, although the static nature of the storage chambers may lead to an eventual build-up of this hormone. The effect is magnified for climacteric fruits, which are known to emit more ethylene during ripening. As a result, ethylene removal technologies offer a way to extend the shelf life of fresh foods while meeting market demands without incurring major economic losses.

The fundamental goal of this work is to produce novel adsorbents based on metals supported on zeolite with the purpose of selective ethylene adsorption. To investigate the role of water in the adsorption processes, the ethylene adsorption performance of synthesized silver and copper metals supported in zeolites with varying characteristics (Si/Al, compensating cation) and metal loadings was studied in dry and wet settings. The best performing metal supported zeolites were shaped through mixing-extrusion, and their performance under wet conditions was compared to the powder samples, as well as the influence of varied zeolite percentages and metal loadings. Furthermore, wet adsorption-desorption cycle studies were performed to investigate the regeneration capacities and their influence on

adsorption performance. In addition, wet adsorption-desorption cycle studies were performed to determine the regeneration capacities and their influence on adsorption performance. Ultimately, the shaped samples were submitted to real (or close to real) conditions adsorption-desorption cycles in a pilot scale adsorption system installed in Rocha-Center's test storage chambers (filled with Rocha Pear fruits) to evaluate the performance capabilities under practical storage conditions.

2.Experimental

2.1 Adsorbent Preparation

NH_4ZSM-5 CBV8014 from Zeolyst (Si/Al=40), NH_4ZSM-5, CBV 3024E Zeolyst (Si/Al=15), sodium nitrate (NaOH, > 98 wt.%) from Sigma-Aldrich, silver nitrate (AgNO3, > 99 wt.%) from ThermoScientific, cupric acetate monohydrate ($Cu(CH_3COO)_2.H_2O$) from Fluka, PURAL SB (Al2O3, 70.3 %) from Condea, *Methocel* from DuPont, nitric acid (10 mol/L) from Merck and ammonium hydroxide (NH_4OH, 25% NH_3) were used as received.

The powder Ag-based ZSM-5 zeolites, used in the experiments were prepared by Ferreira, a PhD student from the Nano4Fresh project.

Two Cu-based zeolites were prepared by ionic exchange. Two different ZSM-5 zeolite parents either ammonium (protonic form after calcination) and sodium form, were used. Since the commercial zeolites available are ammonium-based, the sodium form should be prepared. This synthesis consisted of three one-hour ionic exchanges that were performed to ensure 100% exchange. Each step consisted of exchanging 15 g of NH_4ZSM-5 with 276 mL of a 1 M $NaNO_3$ solution under constant vigorous stirring at room temperature (RT). Between each exchange, the zeolite was recovered by vacuum filtration (ME 1 c vacuum pump from Vacuubrand). After the final exchange, the zeolite was washed with deionized water multiple times before being dried overnight at 80 °C in an oven. Both the Cu-zeolites were prepared by exchanging 8 g of the respective parent zeolite form with 605 mL of a 0.03 M $Cu(CH_3COO)_2.H_2O$ solution under constant vigorous stirring (J.P. SELECTA AGITAMATIC-N) at room temperature during 8 hours. Then the zeolites were recovered by vacuum filtration and dried overnight at 80 °C in an oven. Finally, the powders were subjected to a calcination treatment: 2 °C/min heating ramps, plateaux at 200 °C (for 1 hour) and 500 °C (for 6 hours) under a dry air stream (4 L/h/g).

The zeolite extrudates were prepared by mixing-extrusion method, according to Mendes's[1] procedure with some minor changes The ZSM-5 (Si/Al=40) zeolite was mixed with the pseudo-boehmite and *Methocel* powders. Two mixtures were prepared by varying the zeolite proportion (40%/60% zeolite to dry content and 1% *Methocel).* Firstly, 10 g of the powders were mixed with 5.8 mL of a HNO_3 solution (3.6 wt.%) and 5.4 mL of water was added through the kneading process. After kneading for 15 minutes, 5.9 mL of a NH_4OH solution (1.4 wt.%) was added to the mixture. The kneading of the paste proceeded for about 15 minutes and 5.6 mL of water was added through the process. Cylindrical extrudes were finally obtained by extrusion through a syringe. The alteration made to the documented procedure where the addition of more water (double the amount) to facilitate the extrusion with a syringe. After extrusion, the extrudates were dried at 80 °C overnight in the oven and calcined at 500 °C with a heating rate of 10 °C/min. Calcination was performed on a muffle (Nabertherm). After the heat treatment at 500 °C, the pseudo-boehmite (PURAL SB) transforms into γ-Al_2O_3.[2] After the calcination, the silver-based extrudates were prepared through ionic exchange by adding the appropriate amount of silver precursor solution (silver nitrate on 100 mL) to the extrudates. The process was carried out in a rotary evaporator (BUCHI) with a bath temperature of 40 °C under a vacuum, programmed to evaporate the water, leaving silver deposited in the extrudates. Finally, the silver-loaded extrudates were subjected to another calcination process, under the same conditions as the first one.

2.2 Adsorbents Characterization

Chemical analyses of powder zeolite samples were carried out at the IST Analysis Laboratory employing Inductively Coupled Plasma Optical Emission Spectroscopy (ICP-OES).

UV-Vis DRS spectra were acquired for all materials using a Varian Cary 5000 at room temperature with wavelengths covering from 200 to 800 nm and a Praying Mantis (integration sphere) accessory for DRS measurements. The Kubelka-Munk function was used to transform the reflectance spectra into $F(R) = K/S = (1 - R)2/(2R)$, where K, S, and R represent absorption, scattering, and diffuse reflectance, respectively.

H_2-TPR profiles for all samples were acquired on a micrometrics AutoChem II at 900 °C with a heating rate of 10 °C/min.

N_2 sorption measurements were performed on the shaped samples using a Micromeritics ASAP 2010 analyser and a Quantachrom Autosorb IQ. Prior to analysis, the samples were outgassed under vacuum for 1 hour at 90 °C, then at 350 °C for 5 hours with a 5 °C/min temperature ramp.

Thermogravimetric analysis of powder zeolites was performed in a Setaram SETSYS Evolution with an airflow of 30 mL/min from room temperature to 800 °C.

2.3 Breakthrough curve adsorption experiments

The adsorption process was carried out in a U-shaped fixed bed flow reactor loaded with the adsorbent, immersed in a thermostatic bath (Grant LTD 6) to maintain the temperature (1°C). The feed consisted of a gas flow mixture of ethylene and nitrogen (50 mL/min, 50 ppm of ethylene) controlled by Bronkhorst® gas flow controller. There are 2 three-way valves to alternate between the bypass and the reactor. If the test is conducted under wet conditions, the nitrogen gas is saturated by flowing through a bubble humidifier (filled with de-ionized water) contributing to an RH of 80%. This set is bypassed on the dry condition's experiments. During the adsorption process the reactor gas effluent is analysed in a gas chromatograph (Shimadzu GC-2010 Plus) with a flame ionization detector (FID) with an air

and H_2 flame and N_2 carrier. The signals are then analysed through the LabSolutions software during the experiments. Effluent samples were injected each minute and analyses were performed (LabSolutions software) with the intent to follow the adsorption process. The reactor was filled with a mixture of 100 mg zeolite and 200 mg SiC stabilized between two quartz wool beds for all powder experiments. To prevent diffusional problems, prior to each test, the powder was pelletized with a pressure of 1.5 tons for 30 s. Then, the pellet was crushed and sieved with a particle size between 250-125 µm. In the extrudates testing, 300 mg of extrudates were supported by quartz wool beneath. Prior to each test, the samples were pre-treated *in situ* to remove water and contaminants that had been adsorbed from the saturated samples. This was accomplished by heating the reactor to 250 °C in a ThermoLab oven controlled by a thermocouple (with a heating ramp of 10 °C/min and a 25-minute plateau at 250 °C) with N_2 flow (50 mL/min) for powders and air flow (50 mL/min) for extrudates. The pre-treatment between each cycle for the adsorption-desorption cycling studies was performed by raising the thermostatic bath temperature to 60 °C under air flow (50 mL/min), resulting in the desorption of ethylene and water adsorbed during the adsorption tests.

2.4 Adsorption-desorption experiments under real conditions

The silver-based zeolite extrudates samples were evaluated under real conditions in the Rocha-Center's test chambers. Citicell sensors were used to monitor gas concentrations (O_2, N_2 and C_2H_4) every hour. The concentrations of O_2 and CO_2 gases in the chamber used for these tests are not actively regulated, that is, no precise concentration is specified. However, some control is done since the O_2 (N_2 injection) and CO_2 (CO_2 scrubbers) gas concentrations are kept below certain thresholds. Each chamber holds 90-120 kg of pears (6 boxes of pears) and has a total volume of 592 L (74 cm-80cm-1m). The fundamental principle behind the pilot scale adsorption system is to remove ethylene by recirculating air from the chamber through an active adsorbent (silver-based extrudates) encased in a cartridge. A pump (flow rate 6.8 L/min) is utilized to recycle the gas in the chamber. The incoming gas is then passed through the cartridge (surrounded by aluminium foil), which holds about 3.5 g of extrudates. The ethylene level is measured before and after the cartridge using two sensors (C-10 by Membrapor) connected to a microcontroller. The ethylene concentration data (inlet and outflow) is collected and analysed using the MembraSens 4.0 software. Following each adsorption, the silver-based extrudates samples were thermally treated at 60 °C with an air stream (flow rate 30 L/min) for 30 minutes. The samples were also thermally treated (using the same desorption process) prior to the initial adsorption to eliminate any adsorbed compounds.

3 Results and discussion

3.1 Ag-based adsorbents characterization

The chemical analysis results (Table 1) can be used to infer certain conclusions. Silver cations have a greater affinity than Na^+ and NH_4^+ because they are highly polarizable and hence interact strongly (electrostatically) with the negatively charged zeolite frameworks. [3] Higher Si/Al ratios on the zeolite framework resulted in lower silver loadings for the same ionic exchange procedure. This is because zeolites with a higher aluminium content (lower Si/Al) contain a higher concentration of charge-balancing framework cations (in this example, either H^+ or Na^+), which assure neutrality by compensating for the negative charge produced by the Al atom in the framework. As a result, the silver cationic species (Ag^+) will exchange with the compensating cations contained in the zeolite via ionic exchange.[3]

To guarantee the same load in each adsorption experiment, all samples were kept saturated in other samples. A TGA was used to measure the water loss after pre-treatment. The mass loss was employed to calculate the exact mass of dry zeolite during each experiment. A significant decrease in mass (8%) at 90 °C, can easily be associated with the endothermic evaporation of adsorbed water.

All the Ag-based samples' UV-Vis spectra reveal two main bands at 210 and 225 nm (Figure 1 and Figure 2). According to literature reports[4], these bands have a wavelength in the range of 208-238 nm, which might be attributed to the $4d^{10} \rightarrow 4d^9\ 5s^1$ electronic transition of trigonally coordinated Ag^+ species. [5] The distribution of Ag^+ in different positions inside the cages might explain the two peak positions. The lack of bands at higher wavelengths suggests the absence of the $Ag_n^{\delta+}$ cluster or metallic silver.

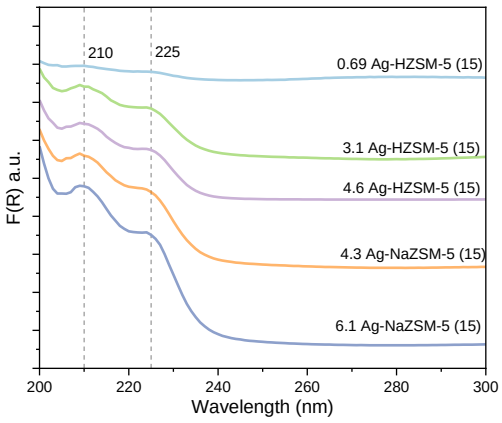

Figure 1- UV-Vis DRS spectra of Ag-based zeolites (Si/Al=15)

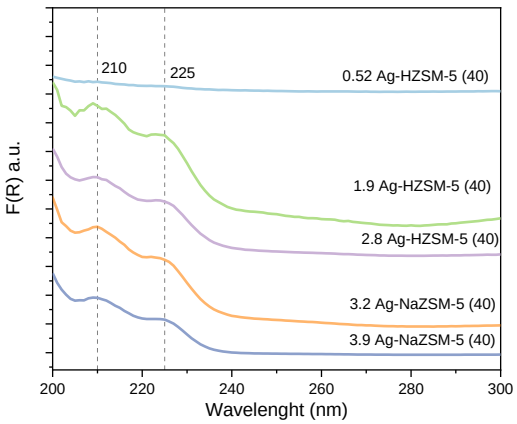

Figure 2- UV-Vis DRS spectra of Ag-based zeolites (Si/Al=40)

Figure 3 and Figure 4 show evidence of two separate reduction bands in the H_2-TPR profiles of the Ag-based powders, associated with the two-step reduction of Ag^+ species. The first is related to the reduction of Ag^+ to $Ag_n^{\delta+}$ clusters while the second is connected with the reduction of $Ag_n^{\delta+}$ cluster into metallic silver. The research conducted by Shibata *et al's*[6] supports these attributions. Furthermore, Shibata *et al.* explored the nature of the clusters formed on MFI structures, concluding that Ag_4^{2+} clusters are the most likely species produced.

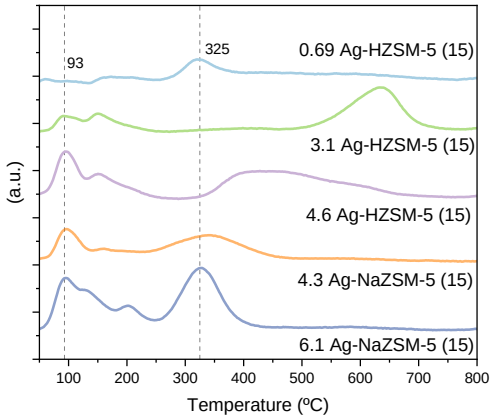

Figure 3-H_2 TPR profile of Ag-based zeolites (Si/Al=15)

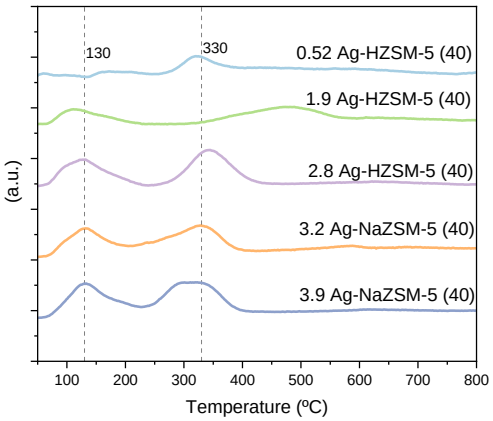

Figure 4 - H_2 TPR profile of Ag-based zeolites (Si/Al=40)

The formed $Ag_n^{\delta+}$ species were considered to be Ag_4^{2+} clusters species (in accordance with the Shibata et al.'s study), and the results are presented in Table 1.

$$4Ag^+ + H_2 \rightarrow {Ag_4}^{2+} + 2H^+ \quad (1)$$

$${Ag_4}^{2+} + H_2 \rightarrow 4Ag^0 + 2H^+ \quad (2)$$

The total amount of Ag^+ species was estimated using equation 1, while the amount of H_2 was obtained by integrating the first peak.

Table 1- H_2-TPR results for the Ag-based zeolites

Sample	Ag (µmol/g) *	Ag^+ (µmol/g)	Ag^+ mol %
0.69 Ag-HZSM-5(15)	64	32	50
3.1 Ag-HZSM-5 (15)	287	183	63
4.6 Ag-HZSM-5 (15)	426	330	77
4.3 Ag-NaZSM-5 (15)	399	218	55
6.1 Ag-NaZSM-5 (15)	566	475	84
0.52 Ag-HZSM-5(40)	48	23	46
1.9 Ag-HZSM-5 (40)	176	138	78
2.8 Ag-HZSM-5 (40)	260	223	86
3.2 Ag-NaZSM-5 (40)	297	221	75
3.9 Ag-NaZSM-5 (40)	362	279	77

*Ag content quantified by ICP-OES

The relationship between the Ag^+ cations (calculated from TPR analysis) and the total silver loading (as determined by chemical studies) is in accordance with the UV-Vis analysis that evidence spectra profiles dominated by Ag^+ species. The overall low number of clusters (either metallic or charged) formed on the ZSM-5 zeolites is expected, since the phenome leading to the formation and growth of zeolites is dependent on the size of the pores, thus medium pores (5.1 x 5.5 Å; 5.3 x 5.6 Å) of ZSM-5 limit the occurrence of these clusters.[3]

In either case, a rise in silver load led to an increase in charged silver species and the proportion between Ag load and Ag^+ species formed appears to be 0.6-0.8.

3.2 Adsorption breakthrough experiments under dry and wet conditions (Ag samples)

The ethylene adsorption performance of the silver-based zeolites under wet and dry conditions was tested and the results are summarized in Figure 6.

Adsorption is dependent on interactions between ethylene and the zeolite, which can be either physical or chemical. The latter one is based on stronger interactions through chemical bond formation, thus more selective and effective interactions are made between ethylene and adsorbent resulting in higher adsorption capacities. A chemisorption mechanism known as π-complexation can occur in the case of silver-based zeolites (as well as other transitional metals), although not all silver species can interact with ethylene in this way. According to Cisneros *et al.*[7] and Horvatits *et al.*[8]charged silver species, such as Ag^+ and $Ag_n^{\delta+}$ clusters, can establish π-interactions with ethylene. Monzón *et al.* [9], on the other hand, found that the silver cluster reduces the number of active sites for ethylene π-interaction and contributes to pore obstruction. Furthermore Horvatits *et al.*[8] determined that silver oxide can also undergo π-complexation with ethylene, however the interaction is less significant, due to the Ag atom's electron deficiency.[10] So, by far, the most significant species in ethylene adsorption are highly dispersed Ag^+ ions. Figure 5 highlights this significance, since greater ethylene adsorption capacities were observed for samples with higher content of Ag^+ species. The findings of Cisneros *et al.* [7] evidences the same impact with the increase of charged silver species content in zeolites.

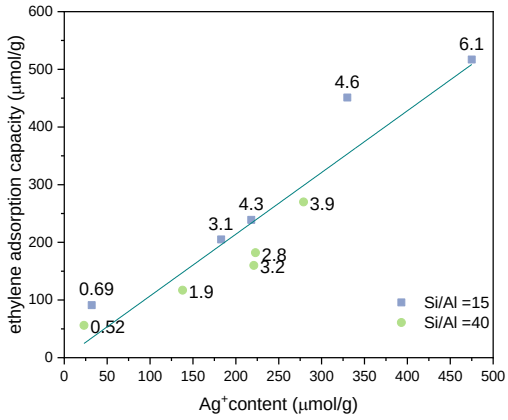

Figure 5- Ethylene adsorption capacity as a function of Ag⁺ content for Ag-based zeolites under dry conditions

According to the trend line depicted in Figure 5, the relationship between the ethylene capacity and Ag^+ content appears to be roughly 1 to 1. As a result, each Ag^+ molecule can adsorb 1 molecule of ethylene. These findings are in accordance with the 1 to 1 verified by Kang *et al.'s* [11]experimental research. Finally, as the increase in capacity is noticeable for each increment in Ag^+ content (evidenced by the sharp trend line), Ag^+ is well dispersed and few silver oxides were formed, as concluded by the H_2 -TPR calculations. These results contrast with Lee *et al.* [10] findings that concluded that the incensement in silver loading results in reduced dispersion of Ag particles, eventually leading to Ag_2O formation.

As shown in Figure 6, these competitive behaviour provoked by water additions led to an significative reduction (about 75%) in adsorption capacity in all samples. This drop in ethylene adsorption under wet conditions was also observed Kang *et al.'s*[11] and Lee *at al.'s*[10] studies, although their experiments were performed under considerable lower RH and higher temperatures.

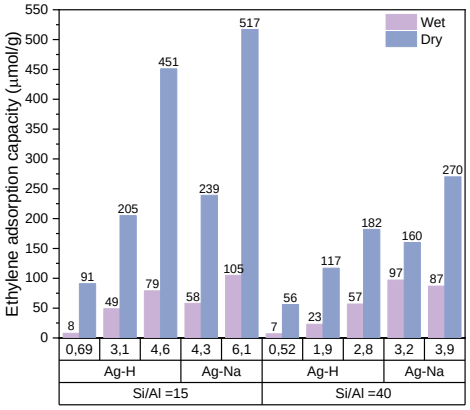

Figure 6 - Comparison of ethylene adsorption capacity for Ag-based zeolites under wet and dry conditions

Figure 7 shows that, despite the wet circumstances, the linear rise in ethylene adsorption capacity with increasing Ag^+ species is still confirmed. However, the lower slope indicates competitive behavior between water and ethylene molecules. The C_2H_4/Ag^+ ratio decreased from 1 up to 0.23 (Si/Al=15) and 0.32 (Si/Al=40), which are in line with Kang *et al.'s*[11] results. Modifying the compensating cation had no discernible effect on the degree of interaction with water. However, increasing the Si/Al ratio improved the zeolite's hydrophobic characteristics (verified by the higher slope), resulting in improved adsorption performance. Chebbi *et al.'s* [3] also detected a rise in hydrophobicity for higher Si/Al ratios. The increase in Ag^+ species is accompanied by an increase in ethylene adsorption capability. According to Tahraoui *et al.'s*[12] work, an increase in highly polarizing species is related to an increase in water affinity via electrostatic interactions. However, as shown in Figure 7 an increase in silver load had no effect on water impact. This phenomenon may be explained by the fact that an increase in silver content resulted in a rise in Ag-charged species (mainly Ag^+), which form stronger connections with ethylene via π-interactions, whereas water contact is associated with physical electrostatic adsorption on Ag sites. The results of Lee *et al.'s*[10] investigation also show that silver has a lower affinity for water.

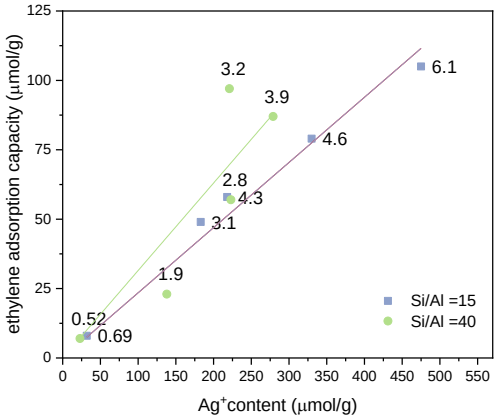

Figure 7- Ethylene adsorption capacity in function of Ag⁺ content for Ag-based zeolites under wet conditions

3.3 Cu-based adsorbents characterization

The UV-Vis spectra of all Cu-based materials show a single wide main band at 780 nm (Figure 8). According to Martins et al.'s [13] findings, this wide band found in the 600-850 nm region might be attributable to Cu^{2+} cations in hexagonal coordination.

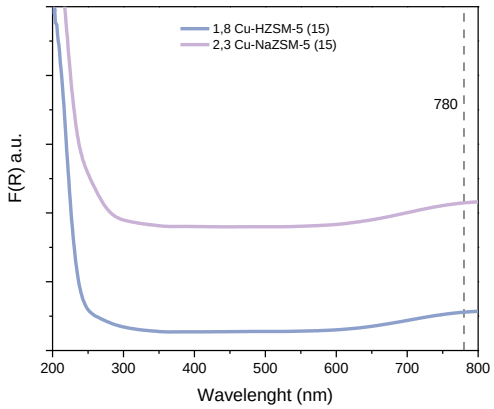

Figure 8- UV-Vis DRS spectra of Cu-based zeolites

H_2 TPR's profiles reveal evidence of two distinct reduction bands in the Cu-based zeolites adsorbents. According to the literature[14], [15], the possible reactions involved in the reduction process are the reduction of CuO into metallic copper (represented by equation 3) or the two-step reduction of Cu^{2+}, comprised by the reduction of Cu^{2+} into Cu^+ at lower temperatures (represented by equation 4)

and the reduction of Cu^+ into metallic copper at higher temperatures (represented by equation 5).

$$CuO + H_2 = Cu^0 + H_2O \quad (3)$$

$$Cu^{2+} + 0.5H_2 = Cu^+ + H^+ \quad (4)$$

$$Cu^+ + 0.5H_2 = Cu^0 + H^+ \quad (5)$$

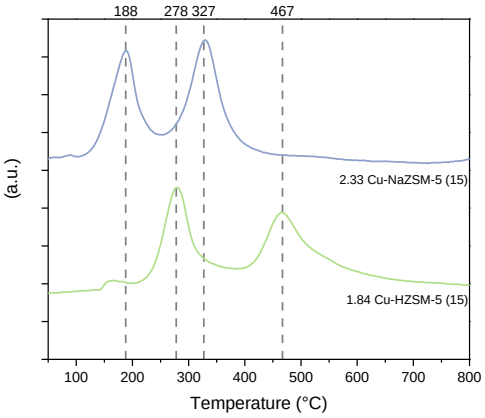

Figure 9- TPR profile of Cu-based zeolites

The TPR profiles of the samples follow a similar pattern, with the second peak area being greater than the first peak area, indicating that the samples contain a minor amount of Cu^+ (presumably created by the pre-treatment).

3.4 Adsorption breakthrough experiments under wet conditions

The ethylene adsorption performance of the copper zeolites under the same wet conditions was tested and compared with the silver-based zeolites.

Table 2- Summary of ethylene capacity values and break-point time for Cu-based zeolites under wet conditions

Sample	q (µmol/g)
2.33 Cu-NaZSM-5(15)	26
1.84 Cu-HZSM-5 (15)	13

*Cu content quantified by ICP-OES

As shown in Table 2, the ethylene adsorption capacity of copper-based zeolites was much lower than that of silver-based zeolites for identical metal loading. This decline can be attributed to how various copper species interact with zeolite, particularly those capable of forming π-complexation bonds with ethylene. Jen *et al.'s* [16] infrared spectroscopy investigation indicated that Cu^+ interacts with ethylene in the same way as Ag^+ does by generating π-complexes. Cu^{2+} interactions with ethylene, on the other hand, are mediated by van der Waals electrostatic forces that are substantially weaker. Furthermore, the bivalent nature of Cu^{2+} cations results in a higher polarization charger, which improves the interaction with water and leads to higher hydration layers. [17], [18]

The decreased adsorption capacity of the copper-based zeolites can be attributed to the prevalence of Cu^{2+} species that are unable of interacting through π-complexation. This is consistent with the findings of Abdi *et al.'s* [19] comparative adsorption studies (between Ag and Cu zeolites), which ascribe the decrease in performance to the presence of Cu^{2+} species. Kim *et al.'s*[20] study on copper zeolite for active cold-start hydrocarbon removal elucidates the critical role of Cu^+ ions in achieving increased adsorption capacities, particularly in wet environments.

3.5 Ag-based extrudates characterization

The textural properties of the extrudates samples were analysed through N_2 adsorption and the results are summarized below.

Table 3- N_2 sorption results and microporosity loss by extrudates with different zeolite loads

Sample	V_{mic}	V_{mic} (theoretical)	V_{mic} loss (%)
HZSM-5 40 (powder)	0.182	---	---
HZSM-5 (40% zeolite)	0.041	0.073	44
HZSM-5 (60% zeolite)	0.090	0.109	17

As seen in Table 3, the extrudates had a significant reduction in microporosity (compared to the zeolite powder) . Because γ-Al_2O_3 is a mesoporous binder, the loss is attributed to alumina agglomeration leading to pore blockage. Adsorption is a diffusion-limited process, therefore increasing the diffusion path and decreasing the accessibility of the active site (a phenomenon known as "binder-blinding") has a significant influence on adsorbent performance.[21], [22]

Extrudates with a greater zeolite content (60%) were prepared in order to reduce this effect. As calculated by the percentage of microporous volume loss, the increase of zeolite in the extrudate (from 40 to 60 wt.%) resulted in less pore obstruction and, as a result, more accessible active sites for ethylene adsorption.

A blank test with extrudates constituted of silver-doped γ-Al_2O_3 was performed to identify the type of species stabilized on this support.

Three prominent bands are visible in the UV-Vis spectra of the silver-based extrudates. The two bands at 210 and 225 nm can be assigned to the electronic transition of trigonally coordinated Ag^+ species, as previously seen in silver-base zeolite powders. [4] The third band presents a maximum at 322 nm and might relate to Ag_n clusters, either neutral or slightly positively charged, which comprise a small amount of Ag atoms, according to Chaieb *et al.'s* [23] research. According to these authors, these species give the samples a fading yellow colour that becomes white after thermal treatment under oxidative conditions. This observation matches the colour change seen in the silver-based extrudates samples after an air pre-treatment prior to the adsorption experiments. [24] The use of pre-treatment gas was made in order to maximize the number of species capable of interacting with ethylene through π-complexation. Following the adjustments, higher adsorption capacities were achieved, demonstrating the worse adsorption capability of Ag_n clusters (either in a neutral or slightly positively charged state). The absence of Ag_2O

particles should not be considered because small silver oxide particles are not detected in UV-Vis DRS spectra.[19]

For the silver loaded alumina sample, the lack of bands in the 210-225 nm range might imply an absence of isolated Ag^+ species, and the band at 250 mn can be attributed to smaller $Ag_n^{\delta+}$ clusters. Furthermore, the presence of Ag^+ bands on zeolite extrudates could imply that these species are stabilized on zeolite active sites.

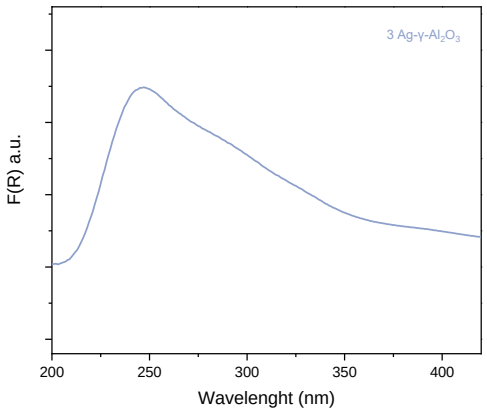

Figure 10- UV-Vis DRS spectra of Ag-based γ-Al_2O_3 extrudates

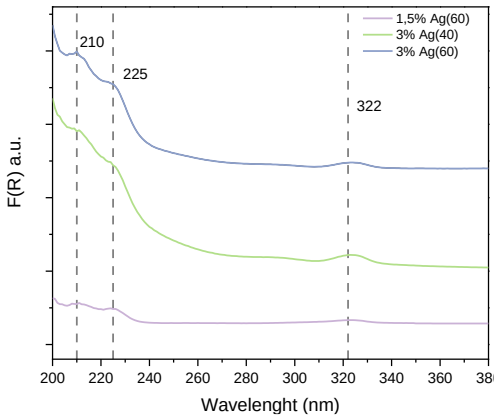

Figure 11- UV-Vis DRS spectra of Ag-based extrudates

The TPR profile for the silver-loaded γ-Al_2O_3 extrudates shows a sharp peck at 110 °C that could be associated with the reduction of Ag_2O to metallic silver. Similar behaviour was evidenced by Son *et al.*[25]for similar concentrations of silver supported in γ-Al_2O_3. The attribution of two less intense peaks is quite dubious since they could be associated with the reduction of Ag^+ species generated by the oxidation of the clusters, as evidenced by the UV-Vis or the decomposition of more dispersed Ag_2O species.[26]

The interpretation of the TPR profiles obtained in Figure 13 is quite complex since there is no information in the literature evidencing the selective deposition of silver in either support (γ-alumina or zeolite). However, the UV-Vis spectra highlighted the presence of Ag^+ isolated species in the extrudates with zeolite (absent in the alumina extrudates) which could suggest the selectivity towards the deposition of silver on the zeolite active sites. These can be corroborated by the existence of two peaks in the TPR profiles, that can be associated with the partial reduction of Ag^+ species to $Ag_n^{\delta+}$ clusters, first, and then $Ag_n^{\delta+}$ cluster into metallic silver.

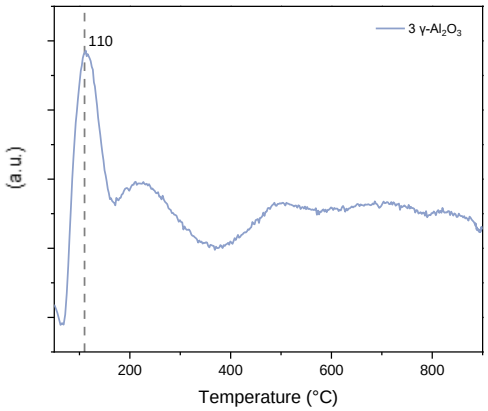

Figure 12-H_2 TPR profile of silver supported in γ-Al_2O_3 extrudates

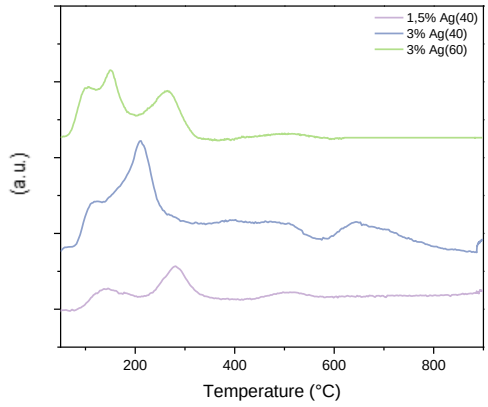

Figure 13- H_2 TPR profile of silver extrudates

3.6 Ag-based extrudates adsorption breakthrough experiments under wet conditions

The ethylene adsorption performance of the ag-based extrudates was tested under wet and the results are summarized in Table 4.

Table 4- Summary of ethylene capacity values and break-point time for Ag-based extrudates under wet conditions

Sample	q (µmol/g extrudates)
3 Ag-γ-Al_2O_3	14
3 Ag(40)	68
1.5 Ag(40)	66
3 Ag(60)	89

As previously indicated, the existing analyses cannot precisely determine the quantity and type of silver species deposited on each support material. Nonetheless, the adsorption capacities may be useful in this respect. The adsorption value of γ-Al_2O_3 extrudates is significantly lower than that of the other samples tested, suggesting that the species stabilized in the support do not interact strongly with ethylene and are most likely undispersed silver oxide clusters. Despite the ability to form π-complexation bonds with ethylene, Lee *et al.'s*[10] research showed that these interactions are significantly weaker (than isolated Ag^+) due to the Ag atom's electron deficiency. Moreover, in the scenario of Ag^+ stabilized in alumina, their contribution to π-complexation would be significantly reduced due to electron density transfer from Ag^+ to the Lewis acid sites of alumina, as demonstrated by Padin *et al.'s*[27] results.

According to this hypothesis, the most active species for ethylene adsorption are found to be the active sites of the zeolite support, most likely the dispersed Ag^+ species shown in the UV-Vis spectra of the extrudates.

Another conclusion is that most of the metallic clusters (neutral or slightly charged) present in the TPR profiles are deposited in the zeolite because changing the pre-treatment gas (N_2 to air) resulted in an increase in adsorption capacity due to the formation of more dispersed active Ag^+ species (oxidation of small metallic clusters) for π-complexation. Jacobs *et al.* [28] identified this phenomenon during thermal treatment tests under moderate oxidative conditions, which resulted in the re-oxidation of internal neutral nanoclusters into dispersed Ag^+ species.

The increase in ethylene adsorption capability is strongly tied to the rise in the extrudates' zeolite percentage. These may be attributed to the decrease in binder agglomeration inside the zeolite pores, which resulted in increased accessibility for stabilization of Ag^+ species. The hypothesis of active silver species being "trapped" inside the clogged micropores was rejected since the ionic exchange happened after the extrusion process. The studies with varied silver loads for the same zeolite percentage provide an unusual outcome. An explanation for the relatively lower difference in capacities could be that the active zeolites sites are fully occupied, and the extra silver is loaded as silver oxide on alumina, but further investigation is needed to validate this hypothesis. Finally, replicability is a crucial characteristic of a technology's scalability. Multiple batches of each zeolite were made and evaluated in this regard. The experimental results for the identical extrudates demonstrated similar adsorption capabilities, ensuring replicability.

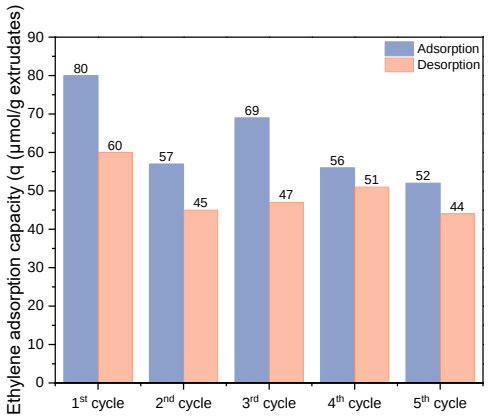

Figure 14- Summary of ethylene capacities for 3Ag(60) extrudates adsorption-desorption cycles tested under dry conditions

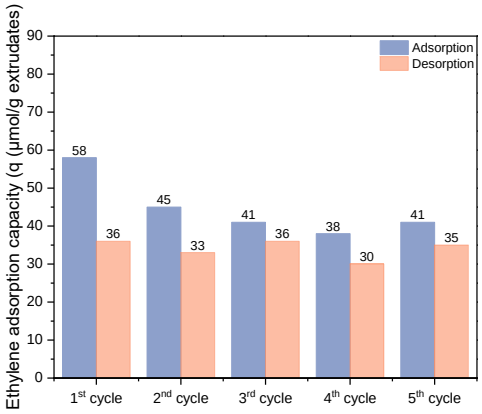

Figure 15- Summary of ethylene capacities for 1.5Ag(40) extrudates adsorption-desorption cycles tested under dry conditions

The adsorption-desorption cycle data (Figure 14 and Figure 15) for the two extrudates studied show comparable patterns. The first cycle has the greatest ethylene adsorption capacity, while the following cycles show a reduction in adsorption performance that is maintained throughout the four cycles. This decrease in performance might be attributed to incomplete ethylene or water desorption. Either compound can interact with the active species at different pore locations, with varying degrees of interaction strength. Consequently, it is extremely conceivable that a non-negligible percentage of the adsorbed compounds require higher temperatures to desorb.

There were no additional declines in adsorption capacities identified in subsequent cycles, implying that there are no large alterations in the active species present in the adsorption process, and so the oligomerization and sintering are most likely discarded. The disparity in adsorption-desorption values for ethylene concentration can be attributed to data losses caused by the adjustment in experimental setup between the adsorption and desorption operations.

3.7 Adsorption-desorption cycles experiments under real conditions

The last part of the work involves testing the extrudates under ''real'' conditions in the Rocha-Center's test chambers. The extrudates were evaluated under real conditions and due to the continually changing nature (VOCs, O_2, CO_2 gas composition, *etc.*) of the fruit storage no direct comparison of performance could be performed. However, a few conclusions may be drawn from the findings, including the recoverability of adsorption capacity following desorption and the selectivity of the adsorbents towards ethylene. All these results provide an excellent

means to assess the viability of these technologies in real-life scenarios (proof of concept).

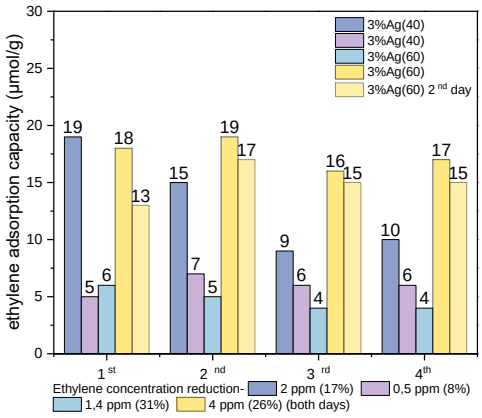

Figure 16- Summary of ethylene adsorption capacity in each cycle and the overall reduction of ethylene concentration

Each adsorption-desorption experiment (Figure 16) shows a significant decrease in ethylene concentration. In general, the extrudates restore their adsorption capacities over the cycles after regeneration. The large changes in ethylene adsorbed between the same sample trials are primarily due to the starting ethylene concentration in the chamber (10-5 ppm). This affects the adsorption process because the difference in concertation is a driving force behind the adsorption process. For comparable baseline ethylene concentrations, increasing the zeolite fraction in the extrudates increases ethylene removal from 8 to 31%.

Preliminarily, it can be noted that the developed adsorbents demonstrated high selectivity for ethylene in an environment including various VOCs and CO_2. The regeneration ability of extrudates is one of the most essential properties since it considerably influences the amount of active medium required for ethylene removal. Despite the various gas compositions, an average ethylene concentration decrease of 16.4% after 8 hours was verified for rather small cartridge loadings of active extrudates (3.5 g). The extrudates showed great mechanical strength, mainly because no significant deterioration was verified even at a substantially high desorption gas flow rate.

Despite the absence of information on gas composition, this comparison further corroborates the importance of an increase in active Ag^+ species in selective ethylene adsorption. The revealed regenerative capacity, together with the low temperature required for desorption, shows the concept's promise as a less expensive and more dependable method of extending fruit shelf-life during storage and transport.

4. Conclusion and future perspectives

The current study aimed to create a novel adsorbent based on metal-loaded zeolites that ensures effective ethylene adsorption, with the goal of controlling the ethylene concentration in industrial fruit storage chambers.

Comparatively, the silver-based zeolite demonstrated superior adsorption performance. This is supported by the highly dispersed Ag^+ species capable of interacting with ethylene via a chemisorption process known as π-complexation. Copper-based zeolites were characterized by the stability of Cu^{2+} species, which interact with ethylene via lower-strength Van der Waals electrostatic interactions, resulting in lower ethylene adsorption performances.

The addition of water to the studies resulted in a considerable decrease in performance (about 75%). This was attributable to competing ethylene and water adsorption in the zeolite, as indicated by a shift in the number of molecules of ethylene adsorbed per Ag^+ active site. In dry conditions, the C_2H_4/Ag^+ ratio was 1, whereas, in wet conditions, the C_2H_4/Ag^+ ratio was 0.23 (Si/Al=15) and 0.32 (Si/Al=40). Concerning the change in properties, higher silver loading was verified for Na-based parent zeolites, and a rise in Si/Al ratio resulted in an improvement in adsorption performance under wet conditions, indicating lower water affinity (more hydrophobic). Overall, an increase in silver loading enhanced ethylene adsorption due to an increased amount of active π-complexation species (Ag^+).

Shaping had a considerable influence on textural properties, which was confirmed by characterization. The decrease of microporosity caused by binder agglomeration has a significant impact on the availability of zeolite sites for stabilizing active Ag^+ species. Silver species were most likely stabilized as Ag_2O species in the alumina support, resulting in a reduced interaction with ethylene. When compared to powder zeolites, a significant drop in performance was observed. The synthesis of extrudates with greater zeolite percentages reduced the loss of microporosity owing to binder agglomeration, resulting in improved ethylene adsorption capabilities. This improvement is due to an increase in zeolite pore space, which is capable of stabilizing Ag^+ species and reducing internal diffusional problems.

The extrudate adsorption-desorption cycles demonstrated the regeneration capability of zeolite adsorption technologies under low-temperature desorption (60 °C). Following an initial decrease in adsorption capacity, performance was maintained during the next four cycles. The first performance decline was attributed to a tiny amount of ethylene that was not desorbed.

Adsorption-desorption investigations using the pilot scale equipment installed in the Rocha-Center's fruit test chambers confirmed the regeneration qualities and efficient adsorption of ethylene under real conditions. After 8 hours, an ethylene concentration drop of 16.4% was observed for relatively tiny cartridge loads of active extrudates (3.5 g). The prepared extrudates have high mechanical strength since no significant degradation was observed even at high desorption gas flow rates.

The current study reveals the potential of zeolite-based adsorption systems in industrial storage systems. Nevertheless, there is still more work to be done. Carbon dioxide is an important gas in CA storage systems; hence its adsorption influence should be examined in the laboratory. Longer adsorption-desorption cycles (either in the laboratory or at the Rocha-Center) might be beneficial when studying the influence on performance in longer studies. Some ideas were formed in the lab scale studies regarding the early decrease in performance throughout the adsorption-desorption cycles, therefore GC-MS analysis

would be valuable to understand the desorption process. Because temperature has a significant influence on the economic landscape of cooling, greater temperatures during transportation might be employed to lessen the economic impact. Understanding the effect of temperature on ethylene adsorption might have a significant impact on the process in this line of thinking. In terms of shaped zeolites, efforts should be directed at mitigating binder agglomeration and determining the selective load of silver on zeolite and alumina using characterization techniques such as scanning transmission electron microscopy. Further studies on the stabilized species in the alumina binder would be necessary to validate the assumptions suggested during the current work.

5. References

[1] P. S. F. Mendes, "Hydroconversion catalysts based on zeolite mixtures, from ideality to reality," Doctoral dissertation, Instituto Superior Técnico, 2017.

[2] A. Hydrates, "PURAL CATAPAL".

[3] M. Chebbi, B. Azambre, L. Cantrel, M. Huve, and T. Albiol, "Influence of structural, textural and chemical parameters of silver zeolites on the retention of methyl iodide," *Microporous and Mesoporous Materials*, vol. 244, pp. 137–150, May 2017, doi: 10.1016/J.MICROMESO.2017.02.056.

[4] L. Cisneros, F. Gao, and A. Corma, "Silver nanocluster in zeolites. ADSORPTION of ETHYLENE traces for fruit preservation," *Microporous and Mesoporous Materials*, vol. 283, pp. 25–30, Jul. 2019, doi: 10.1016/J.MICROMESO.2019.03.032.

[5] R. Seifert, A. Kunzmann, and G. Calzaferri, "The Yellow Color of Silver-Containing Zeolite A**," *Angew. Chem. Int. Ed*, vol. 37, no. 11, 1998, doi: 10.1002/(SICI)1521-3773(19980619)37:11.

[6] J. Shibata *et al.*, "Structure of active Ag clusters in Ag zeolites for SCR of NO by propane in the presence of hydrogen," *J Catal*, vol. 227, no. 2, pp. 367–374, Oct. 2004, doi: 10.1016/J.JCAT.2004.08.007.

[7] L. Cisneros, F. Gao, and A. Corma, "Silver nanocluster in zeolites. ADSORPTION of ETHYLENE traces for fruit preservation," *Microporous and Mesoporous Materials*, vol. 283, pp. 25–30, Jul. 2019, doi: 10.1016/J.MICROMESO.2019.03.032.

[8] C. Horvatits, D. Li, M. Dupuis, E. A. Kyriakidou, and E. A. Walker, "Ethylene and Water Co-Adsorption on Ag/SSZ-13 Zeolites: A Theoretical Study," *Journal of Physical Chemistry C*, vol. 124, no. 13, pp. 7295–7306, Apr. 2020, doi: 10.1021/ACS.JPCC.0C00849/ASSET/IMAGES/LARGE/JP0C00849_0007.JPEG.

[9] J. D. Monzón *et al.*, "Ethylene adsorption onto thermally treated AgA-Zeolite," *Appl Surf Sci*, vol. 542, p. 148748, Mar. 2021, doi: 10.1016/J.APSUSC.2020.148748.

[10] J. Lee, K. Giewont, J. Chen, C. H. Liu, E. A. Walker, and E. A. Kyriakidou, "Ag/ZSM-5 traps for C2H4 and C7H8 adsorption under cold-start conditions," *Microporous and Mesoporous Materials*, vol. 327, p. 111428, Nov. 2021, doi: 10.1016/J.MICROMESO.2021.111428.

[11] S. B. Kang, C. Kalamaras, Vemuri Balakotaiah, and W. Epling, "Hydrocarbon Trapping over Ag-Beta Zeolite for Cold-Start Emission Control," *Catal Letters*, vol. 147, pp. 1355–1362, 2044, doi: 10.1007/s10562-017-2044-2.

[12] Z. Tahraoui, H. Nouali, C. Marichal, P. Forler, J. Klein, and T. J. Daou, "Influence of the Compensating Cation Nature on the Water Adsorption Properties of Zeolites," *Molecules 2020, Vol. 25, Page 944*, vol. 25, no. 4, p. 944, Feb. 2020, doi: 10.3390/MOLECULES25040944.

[13] L. Martins, R. P. S. Peguin, and E. A. Urquieta-González, "Cu and Co exchanged ZSM-5 zeolites: activity towards no reduction and hydrocarbon oxidation," *Quim Nova*, vol. 29, no. 2, pp. 223–229, 2006, doi: 10.1590/S0100-40422006000200009.

[14] S. J. Gentry, N. W. Hurst, and A. Jones, "Temperature programmed reduction of copper ions in zeolites," *Journal of the Chemical Society, Faraday Transactions 1: Physical Chemistry in Condensed Phases*, vol. 75, pp. 1688–1699, 1979, doi: 10.1039/F19797501688.

[15] J. Sárkány, J. L. d'Itri, and W. M. H. Sachtler, "Redox chemistry in excessively ion-exchanged Cu/Na-ZSM-5," *Catal Letters*, vol. 16, no. 3, pp. 241–249, Sep. 1992, doi: 10.1007/BF00764336.

[16] H. W. Jen and K. Otto, "Chemisorption of alkenes on copper-exchanged ZSM-5 zeolite," *Catal Letters*, vol. 26, no. 1–2, pp. 217–225, Mar. 1994, doi: 10.1007/BF00824047/METRICS.

[17] Y. Marcus, "A simple empirical model describing the thermodynamics of hydration of ions of widely varying charges, sizes, and shapes," *Biophys Chem*, vol. 51, no. 2–3, pp. 111–127, Aug. 1994, doi: 10.1016/0301-4622(94)00051-4.

[18] B. Hribar, N. T. Southall, V. Vlachy, and K. A. Dill, "How ions affect the structure of water," *J Am Chem Soc*, vol. 124, no. 41, pp. 12302–12311, Oct. 2002, doi: 10.1021/JA026014H/ASSET/IMAGES/LARGE/JA026014HF00012.JPEG.

[19] H. Abdi, H. Maghsoudi, and V. Akhoundi, "Adsorption properties of ion-exchanged SSZ-13 zeolite for ethylene/ethane separation," *Fluid Phase Equilib*, vol. 546, Oct. 2021, doi: 10.1016/J.FLUID.2021.113171.

[20] J. Kim *et al.*, "A Cu-impregnated ZSM-5 zeolite for active cold start hydrocarbon removal: Cation-type-dependent Cu species and their synergetic HC adsorption/oxidation functions," *Chemical Engineering Journal*, vol. 430, p. 132552, Feb. 2022, doi: 10.1016/J.CEJ.2021.132552.

[21] N. Wakao and J. M. Smith, "Diffusion in catalyst pellets," *Chem Eng Sci*, vol. 17, no. 11, pp. 825–834, Nov. 1962, doi: 10.1016/0009-2509(62)87015-8.

[22] S. Schwarz, M. Kojima, and C. T. O'Connor, "Effect of stirring, extrusion and pelletisation on high pressure propene oligomerisation and xylene isomerisation over ZSM-5," *Appl Catal*, vol. 68, no. 1, pp. 81–96, Jan. 1991, doi: 10.1016/S0166-9834(00)84095-6.

[23] T. Chaieb *et al.*, "On the origin of the changes in color of Ag/Al2O3 catalysts during storage," *Research on Chemical Intermediates*, vol. 45, no. 12, pp. 5877–5905, Dec. 2019, doi: 10.1007/s11164-019-04007-8.

[24] S. Pal, G. D.-M. R. Bulletin, and undefined 2009, "Reversible transformations of silver oxide and metallic silver nanoparticles inside SiO2 films," *Elsevier*.

[25] I. H. Son, M. C. Kim, H. L. Koh, and K. L. Kim, "On the promotion of Ag/γ-Al2O3 by Cs for the SCR of NO by C3H6," *Catal Letters*, vol. 75, no. 3–4, pp. 191–197, Sep. 2001, doi: 10.1023/A:1016796022644/METRICS.

[26] M. C. Kung and H. H. Kung, "Lean NOcursive greek chi catalysis over alumina-supported catalysts," *Top Catal*, vol. 10, no. 1–2, pp. 21–26, 2000, doi: 10.1023/A:1019147630269/METRICS.

[27] J. Padin and R. T. Yang, "New sorbents for olefin/paraffin separations by adsorption via π-complexation: synthesis and effects of substrates," *Chem Eng Sci*, vol. 55, no. 14, pp. 2607–2616, Apr. 2000, doi: 10.1016/S0009-2509(99)00537-0.

[28] P. A. Jacobs, "Chapter 8 Metal Clusters and Zeolites," *Stud Surf Sci Catal*, vol. 29, no. C, pp. 357–414, Jan. 1986, doi: 10.1016/S0167-2991(08)65379-3.